Published in final edited form as:
Cell Metab. 2014 October 7; 20(4): 626–638. doi:10.1016/j.cmet.2014.09.001.

Let-7 coordinately suppresses components of the amino acid sensing pathway to repress mTORC1 and induce autophagy

Amy N. Dubinsky[1,*], **Somasish Ghosh Dastidar**[1,*], **Cynthia L. Hsu**[1,*], **Rabaab Zahra**[1,#,*], **Stevan Djakovic**[1,^], **Sonia Duarte**[2], **Christine C. Esau**[3], **Brian Spencer**[4], **Travis D. Ashe**[1], **Kimberlee M. Fischer**[3], **Deidre A. MacKenna**[3], **Bryce L. Sopher**[5], **Eliezer Masliah**[4], **Terry Gaasterland**[6,7], **B. Nelson Chau**[3], **Luis Pereira de Almeida**[2,8], **Bradley E. Morrison**[1], and **Albert R. La Spada**[1,4,7,9,10,11,12]

[1]Department of Pediatrics, University of California, San Diego; La Jolla, CA 92093, USA

[2]CNC-Center for Neuroscience and Cell Biology, University of Coimbra, Largo Marquês de Pombal,3004-517 Coimbra, Portugal

[3]Regulus Therapeutics, 3545 John Hopkins Court, Suite 210, San Diego, CA 92121, USA

[4]Department of Neurosciences, University of California, San Diego; La Jolla, CA 92093, USA

[5]Department of Neurology, University of Washington, Seattle, WA 98195, USA

[6]Scripps Institute for Oceanography, University of California, San Diego; La Jolla, CA 92093, USA

[7]Institute for Genomic Medicine, University of California, San Diego; La Jolla, CA 92093, USA

[8]Faculty of Pharmacy, University of Coimbra, 3000-548 Coimbra, Portugal

[9]Department of Cellular & Molecular Medicine, University of California, San Diego; La Jolla, CA 92093, USA

[10]Division of Biological Sciences, University of California, San Diego; La Jolla, CA 92093, USA

Corresponding author: Albert La Spada, MD, PhD, Pediatrics and Cellular & Molecular Medicine, University of California, San Diego, 9500 Gilman Drive, MC 0642, La Jolla, CA 92093-0642, (858)-246-0148 [ph.], alaspada@ucsd.edu.
[#]Present address: Department of Microbiology, Quaid-i-Azam University, Islamabad 45320, Pakistan
[^]Present address: Department of Molecular Oncology, Genentech, Inc., South San Francisco, CA 94080, USA
[*]These authors contributed equally to this work.

Accession Numbers
The microarray data sets can be retrieved from the GEO database: accession number GSE60452.

Supplemental Information
Supplemental information includes Supplemental Experimental Procedures, Supplemental References, one Supplemental Table, and seven Supplemental Figures with legends.

Author contributions
A.N.D., S.G.D., C.C.E., E.M., T.G., B.N.C., B.E.M., L.P.A. & A.R.L. designed the experiments. A.N.D., S.G.D., R.Z., C.L.H., S.D., S.D., B.S., T.D.A., K.M.F., D.A.M., B.E.M. & B.L.S. performed the experiments. A.N.D., S.G.D., C.L.H., R.Z. & A.R.L. wrote the manuscript.

[11]Sanford Consortium for Regenerative Medicine, University of California, San Diego; La Jolla, CA 92093, USA

[12]Rady Children's Hospital, San Diego, CA 92123, USA

SUMMARY

Macroautophagy (hereafter autophagy) is the major pathway by which macromolecules and organelles are degraded. Autophagy is regulated by the mTOR signaling pathway – the focal point for integration of metabolic information, with mTORC1 playing a central role in balancing biosynthesis and catabolism. Of the various inputs to mTORC1, the amino acid sensing pathway is among the most potent. Based upon transcriptome analysis of neurons subjected to nutrient deprivation, we identified *let-7* microRNA as capable of promoting neuronal autophagy. We found that *let-7* activates autophagy by coordinately down-regulating the amino acid sensing pathway to prevent mTORC1 activation. *Let-7* induced autophagy in the brain to eliminate protein aggregates, establishing its physiological relevance for *in vivo* autophagy modulation. Moreover, peripheral delivery of *let-7* anti-miR repressed autophagy in muscle and white fat, suggesting that *let-7* autophagy regulation extends beyond CNS. Hence, *let-7* plays a central role in nutrient homeostasis and proteostasis regulation in higher organisms.

INTRODUCTION

Autophagy is the major eukaryotic cellular pathway by which macromolecules and organelles are degraded (Shintani and Klionsky, 2004). Autophagy involves the initial formation of an isolation membrane, the phagophore, followed by engulfment of cytosolic components and organelles into double membrane-bound vesicles that ultimately fuse with lysosomal compartments to permit degradation of the enclosed contents. Much of what we know about autophagy regulation and the autophagy pathway comes from work done in yeast (Mizushima et al., 1998; Scott et al., 1996). Although mammals also use autophagy as a cellular survival mechanism when faced with starvation conditions, autophagy has been adapted to perform a wide range of functions in higher organisms, including immune response to pathogen invasion, surveillance against cancer, and maintenance of protein and organelle quality control in the CNS (Mizushima and Komatsu, 2011).

Autophagy activation is tightly regulated in the cell based upon nutrient availability and cell stress. As the mTOR signaling pathway serves as a focal point for integration of metabolic information, growth factor signaling, and stress, the principal arbiter of autophagy pathway activity is the mTORC1 complex (Ganley et al., 2009; Hosokawa et al., 2009), though autophagy can also be subject to mTORC1-independent regulation (Lipinski et al., 2010). Under conditions of abundant nutrients and absence of cell stress, mTORC1 directly phosphorylates and thereby inactivates Atg1 (ULK1), which is in complex with Atg13 and FIP200, key upstream autophagy pathway proteins that initiate autophagy induction (Boya et al., 2013). Recent studies have further demonstrated that sensing of nutrient status by the mTORC1 complex is accomplished by direct association with the lysosome, where nutrient availability both within this organelle and in the cytosol is transduced to the mTORC1 complex through a set of signaling complexes that converge on mTORC1 to determine its

activation state (Yan and Lamb, 2012). In addition to autophagy proteins required for the initiation of phagophore assembly, mTORC1 dictates the activity of a master regulatory transcription factor, known as transcription factor EB (TFEB), by phosphorylating TFEB at the lysosome (Roczniak-Ferguson et al., 2012; Settembre et al., 2012), and thereby preventing TFEB entry into the nucleus, where TFEB binds to the promoters of genes required for lysosome assembly, lysosome enzyme production, and autophagosome construction (Settembre et al., 2011).

In light of its numerous essential roles in cellular homeostasis, we hypothesized that autophagy would be subject to sophisticated transcriptional regulatory control, not just downstream of mTORC1, but also upstream of mTORC1 to facilitate integration of nutrient sensing information coming from a variety of signaling pathway sources. We predicted that such fine-tuned regulation would be particularly important in the CNS, where autophagy-mediated turnover of misfolded proteins and damaged organelles guards against disruption of crucial cellular processes. To delineate pathways of genetic regulation of autophagy in the CNS, we developed a novel culture system for autophagy induction in primary cortical neurons (Young et al., 2009), and we used this system to interrogate gene expression changes that occur upon nutrient deprivation mediated autophagy induction. This analysis included evaluation of microRNA expression changes, as we found that Dicer is required for neuronal autophagy, and yielded up-regulation of microRNAs belonging to the *let-7* family as a feature of autophagy pathway activation in primary neurons. We then determined that *let-7* activates neuronal autophagy by repressing the expression of genes that comprise a recently delineated amino acid sensing pathway (Jewell et al., 2013), and confirmed the physiological significance of this *let-7* regulation by documenting *let-7* modulation of autophagy in the brain and in peripheral tissues in mice. These findings reveal a central role for *let-7* in the regulation of cellular metabolic processes.

RESULTS

MicroRNA *let-7* is a potent regulator of neuronal autophagy

To identify the transcriptional basis of autophagy pathway regulation in neurons, we established a system for autophagy induction in primary cortical neurons obtained from GFP-LC3 transgenic mice (Young et al., 2009). This system is based upon culturing GFP-LC3 neurons in a nutrient-limited media (NLM), as LC3 incorporation into autophagosomes, which are formed upon autophagy pathway induction, requires a processing – conjugation step that converts diffuse-appearing GFP-LC3-I into discrete GFP-LC3-II puncta (Klionsky et al., 2012). The conversion of LC3-I to LC3-II can also be monitored by Western blot analysis, as LC3-II migrates at a lower molecular mass than LC3-I (Klionsky et al., 2012). As microRNAs (miRNAs) are enriched in the nervous system and coordinate the regulation of essential processes (Fineberg et al., 2009), we examined if miRNA production is required for neuronal autophagy activation by knocking down Dicer in NLM-cultured GFP-LC3 primary neurons. Transfection of Dicer siRNA into GFP-LC3 primary neurons yielded ~70% reduction in Dicer expression (Figure S1A), and prevented autophagy induction in primary neurons subjected to nutrient deprivation (Figure 1A and S1B), indicating that miRNA production is required for neuronal autophagy. To identify the

miRNAs necessary for neuronal autophagy induction, we performed a miRNA array analysis, comparing GFP-LC3 neurons cultured under normal complete media (CM) conditions and NLM conditions. We identified 19 miRNAs with a fold change of >1.2 at a *P* value of <0.005 and false discovery rate of <0.10 (Table S1). Among these 19 miRNAs, five were members of the *let-7* miRNA family (Roush and Slack, 2008). As Argonaute-2 (Ago) HITS-CLIP analysis of postnatal day 13 mouse cortex established that *let-7* is highly abundant in this brain region (Chi et al., 2009), and therefore likely to be physiologically relevant for neuronal autophagy regulation, we focused on *let-7*, after RT-PCR analysis confirmed increased *let-7* expression in NLM-cultured primary neurons (Figure S1C). Transfection of *let-7* mimic into CM-cultured GFP-LC3 neurons yielded marked autophagy activation (Figure 1B), suggesting that expression of *let-7* is sufficient to induce neuronal autophagy. To assess if autophagy induction is accompanied by proper progression of the autophagy pathway, we treated GFP-LC3 neurons, cultured under normal CM conditions, with *let-7* mimic and found that LC3-II increased relative to actin (Figure 1C, Figure S1D). To determine the flux through the autophagic pathway, we examined the effect of *let-7* mimic in the presence or absence of ammonium chloride, a lysosomal inhibitor, and observed increased autophagy flux upon *let-7* mimic treatment in comparison to treatment with control miR (Figure 1C–D). Analysis of GFP-LC3 puncta formation in primary neurons transfected with *let-7* mimic independently corroborated autophagy induction by *let-7* (Figure 1E and S1E).

let-7 represses the mTOR signaling pathway in neurons without turning off the insulin signaling pathway

The mTORC1 complex is a key sensor of nutrient status, and when activated, mTORC1 promotes protein synthesis, lipogenesis, and energy metabolism, but inhibits autophagy (Laplante and Sabatini, 2012). Primary neurons subjected to nutrient deprivation exhibit autophagy activation in the context of mTORC1 inhibition, as NLM-treated neurons display reduced mTOR phosphorylation (Young et al., 2009). Studies of NLM-treated neurons indicate that suppression of the insulin signaling pathway accounts for mTORC1 inactivation, as NLM-treated neurons exhibit reduced Akt phosphorylation (Young et al., 2009). To determine how *let-7* promotes autophagy induction, we treated primary neurons, cultured under normal CM conditions, with *let-7* mimic or scrambled control mimic, and performed immunoblot analysis of total mTOR and phospho-mTOR. We found that phospho-mTOR, relative to total mTOR, was markedly reduced in *let-7* treated primary neurons and NLM-treated primary neurons (Figure 2A). Immunoblotting of total S6 kinase 1 (S6K1) and phospho-S6K1 confirmed that *let-7*, as well as NLM nutrient deprivation, yields mTORC1 inactivation (Figure 2B), indicating that *let-7* mediates autophagy activation in a mTOR-dependent manner. To evaluate the role of the insulin signaling pathway in mTORC1 inhibition, we examined total Akt and phospho-Akt. Intriguingly, *let-7* treated neurons displayed high levels of phospho-Akt, although NLM cultured neurons exhibited low levels (Figure 2C). To confirm these findings, we performed loss-of-function studies by treating NLM-cultured neurons with anti-*let-7* or with scrambled anti-miR, and then repeated the immunoblot analysis of mTOR, S6K1, and Akt activation status. Nutrient-deprived primary neurons treated with anti-*let-7* displayed increased phospho-activation of mTOR and S6K1 in comparison to NLM controls (Figure 2D–E), as well as increased Akt

phosphorylation (Figure 2F), indicating that, in the neuronal milieu, *let-7* represses mTORC1 activation without suppressing the insulin-signaling pathway.

The amino acid sensing pathway is coordinately repressed by *let-7*

To determine how *let-7* represses mTORC1 activation in neurons, we considered the targets of *let-7* identified by Ago HITS-CLIP analysis of mouse cortex (Chi et al., 2009), and noted that *Slc7a5* was found to be a *let-7* target (Figure 3A). Slc7a5 is part of a bidirectional amino acid transporter that exchanges intracellular glutamine for extracellular leucine to promote mTORC1 activation (Nicklin et al., 2009), and has emerged as a key step in the amino acid sensing pathway (Sancak et al., 2008), that strongly regulates the mTORC1 complex at the lysosome (Jewell et al., 2013). Indeed, mTORC1 remains sensitive to amino acid status even when the insulin signaling pathway is engaged, as in the absence of the negative mTORC1 regulators TSC1 or TSC2 (Smith et al., 2005). TargetScan 6.0 analysis of the 3' UTR regions of 14 genes encoding components of the amino acid sensing pathway yielded predicted *let-7* binding sites for three members of this pathway: Map4k3, RagC, and RagD (Figure 3A). When compared to the number of predicted *let-7* binding sites called by TargetScan for all annotated genes, the fraction of *let-7* sites predicted by TargetScan for the amino acid sensing pathway represents a significant level of enrichment ($P < 10^{-2}$, χ^2 analysis). TargetScan algorithm prediction is restricted to the 3' UTR, but certain studies underscore the potential role of non-3' UTR sequences in miRNA expression regulation (Chi et al., 2009); hence, we examined mRNAs of amino acid sensing pathway components for *let-7* seed site matches and found putative *let-7* binding sites in 13 of 14 components (Figure S2), with many sites falling within coding sequences (Figure 3A). To evaluate putative *let-7* binding sites as potential direct *let-7* targets, we cloned either 3' UTR sequences or coding sequences downstream of a luciferase cDNA, and then measured luciferase activity off of these 13 luciferase reporter constructs, when individually transfected into HEK293T cells in the presence of mature *let-7* duplex or a scrambled miRNA. We observed significant repression of luciferase activity by *let-7* for 3'-UTR fragments or coding sequence fragments for 11 of 13 amino acid sensing pathway components, and a trend toward suppression in the remaining two pathway members (Figure 3B). We introduced mismatch mutations into predicted seed sites for a subset of *let-7* targets, and found that these binding site substitutions abrogated *let-7* suppression of luciferase activity for all four tested amino acid sensing pathway components (Figure 3B).

To further assess the physiological significance of *let-7* repression of amino acid sensing pathway gene expression, we generated a lentivirus expression construct encoding *let-7* or a scrambled miRNA, and infected primary cortical neurons with either *let-7* lentivirus or miR-scrambled lentivirus. After confirming successful, modest induction of *let-7* expression in infected neurons (Figure S3A), we measured expression levels of amino acid sensing pathway genes in neurons infected with *let-7* or the scrambled miRNA, and detected decreased expression for most amino acid sensing pathway genes, with significant reductions noted for a majority of tested genes (Figure 3C). These results indicate that *let-7* is directly and coordinately targeting genes that comprise the amino acid sensing pathway, upstream of the mTORC1 complex. Suppression of amino acid sensing pathway components also occurs when primary neurons are subjected to NLM nutrient deprivation

(Figure S3B). To confirm that *let-7* regulation of amino acid sensing pathway genes occurs at the level of protein expression, we treated Neuro2a cells or primary neurons with a *let-7* anti-miR or scrambled anti-miR, and observed prominent de-repression of putative *let-7* targets upon immunoblotting (Figures 4A and S3C). Quantification of protein expression levels of these *let-7* targets confirmed significant increases, when Neuro2a cells or primary neurons were subjected to anti-*let-7* treatment (Figure 4B and S3D). These findings independently validate the RNA expression level alterations obtained upon *let-7* treatment, and further demonstrate that *let-7* is regulating amino acid sensing pathway genes.

To determine if *let-7* is required for mTORC1-dependent neuronal autophagy induction, we treated NLM-cultured neurons with anti-*let-7* or with scrambled anti-miR, and observed a significant decrease in LC3-II levels in neurons subjected to *let-7* inhibition (Figure 4C). To evaluate flux through the autophagic pathway, we examined the effect of anti-*let-7* on LC3-II levels in the presence or absence of a lysosomal inhibitor, and observed decreased autophagy flux upon anti-*let-7* mimic treatment (Figure 4C–D). We also examined the role of *let-7* in neuronal autophagy induced by amino acid deprivation by subjecting primary cortical neurons, treated with anti-*let-7* or scrambled anti-miR, to amino acid starvation. We again observed a marked reduction in LC3-II levels in neurons subjected to *let-7* inhibition (Figure S3E), and noted decreased autophagy flux upon anti-*let-7* treatment in comparison to treatment with control anti-miR (Figure S3F), confirming the necessity of *let-7* for mediating neuronal autophagy activation during amino acid starvation.

To determine if *let-7*-mediated autophagy activation is upstream to mTORC1 complex repression, we cultured primary cortical neurons under normal CM conditions, infected these neurons with lentivirus encoding the constitutively active Rheb Q64L mutant (Inoki et al., 2003), and transfected these neurons with the GFP-LC3-mCherry reporter construct, in combination with *let-7* mimic or a scrambled miR. We observed prominent autophagic puncta formation in mock-infected primary neurons treated with *let-7*, comparable to the autophagic puncta formation observed in primary neurons subjected to amino acid starvation (Figures 4E and S4). However, expression of Rheb-Q64L dramatically suppressed autophagic puncta formation in neurons subjected to amino acid starvation or *let-7* mimic treatment (Figures 4E–G and S4), indicating that *let-7* activation is mTORC1-dependent. Immunoblot analysis independently confirmed that *let-7* mediated autophagy activation was markedly blunted in the presence of the Rheb-Q64L mutant (Figure 4H–I).

Inhibition of individual *let-7* target genes is sufficient to induce autophagy in neurons

The mTORC1 complex is principally responsible for repression of autophagy pathway activation under conditions of abundant nutrients and absence of cell stress. A defining feature of miRNA transcriptional control of biological processes is the coordinate down-regulation of multiple targets on the same pathway (Small and Olson, 2011), and evaluation of *let-7* regulation indicates that *let-7* promotes neuronal autophagy activation through simultaneous down-regulation of multiple amino acid sensing pathway targets (Figures 3 and S2). However, to assess the physiological relevance of identified *let-7* targets for autophagy control in neurons, where amino acid sensing pathway regulation is yet to be studied, we considered the *let-7* family seed site sequence (Figure 5A), and determined the

extent of *let-7* seed site conservation for genes encoding components of the amino acid sensing pathway. This analysis revealed perfect conservation between mammalian species for one confirmed *let-7* target site in the RagD gene (Figure 5B), and conservation down to zebrafish or frog respectively for two confirmed *let-7* target sites in the Map4k3 gene (Figure 5B), indicating likely regulatory significance; hence, we selected these two targets and individually knocked down each target under nutrient replete CM conditions to examine their role in neuronal autophagy regulation. Upon RagD siRNA knockdown in CM-cultured GFP-LC3 primary neurons, we observed an increased number of GFP-LC3 puncta (Figure 5D–E), which is suggestive of autophagy induction, as observed upon repression of this pathway in a non-neuronal context (Efeyan et al., 2013; Kim et al., 2008; Nicklin et al., 2009). As a block in autophagy pathway progression could be misinterpreted as autophagy induction, we evaluated autophagic flux in nutrient replete Neuro2a cells expressing GFP-LC3-mCherry (Figure S5A), confirmed significant RagD knock-down (Figure S5B), and found that RagD knock-down yielded a marked increase in autophagosomes and autolysosomes (Figure S5C–D), indicative of autophagosome maturation and lysosomal fusion. Map4k3 knockdown in GFP-LC3 primary cortical neurons similarly yielded marked induction of autophagy at levels comparable to nutrient deprivation (Figure 5F–G). To assure that Map4k3 knock-down resulted in autophagy pathway progression, we performed LC3 immunoblotting analysis on primary neurons transfected with Map4k3 shRNA or control scrambled shRNA, confirmed successful Map4k3 knock-down (Figure S6A), and cultured these neurons in the absence or presence of the lysosomal inhibitor ammonium chloride. Characteristic upregulation of autophagic flux was noted for control neurons subjected to nutrient deprivation, and a marked increase in autophagic flux was measured for primary neurons knocked-down for Map4k3 (Figure 6A–B). LC3 Western blot analysis of nutrient replete Neuro2a cells subjected to Map4k3 knock-down similarly resulted in autophagy induction at levels comparable to nutrient deprivation (Figure S6B–C), establishing the importance of amino acid sensing pathway regulation for autophagy in neurons.

In vivo modulation of *let-7* in mice yields activation and repression of autophagy

To evaluate the effect of *let-7* on autophagy pathway function in an *in vivo* setting, we performed stereotactic injections of lentivirus encoding either *let-7* or a scrambled miR (mir-scr) into the striatum of adult wild-type C57BL/6J mice (Figure 6C). As determination of autophagy pathway status *in vivo* is complicated, we chose to co-inject lentivirus containing a human transgene carrying a mutant ataxin-3 cDNA with 72 CAG repeats (Figure 6C), as this encodes a toxic misfolded protein product, which accumulates in aggregates in the brains of patients with spinocerebellar ataxia type 3 (Paulson et al., 1997), and can be removed by autophagy (Nascimento-Ferreira et al., 2013). LC3 immunoblot analysis of protein lysates from the brains of injected mice revealed increased levels of LC3-II relative to actin in striatal samples corresponding to the *let-7* injected hemisphere (Figure 6D–E), suggesting increased autophagy pathway activation. We then obtained sections of striatum from these injected mice, counted the total number of ubiquitin-positive aggregates in regions matched for size and transduction, and observed a dramatic reduction (>50%) in the brains of mice co-injected with *let-7* lentivirus (Figure 6F–G). These results indicate that

let-7 can activate autophagy in the mammalian brain and promote increased turnover of a misfolded protein in mouse CNS.

To test if *in vivo let-7* inhibition would repress autophagy in the CNS, we performed intracerebroventricular injections of anti-*let-7* on adult C57BL/6J mice and completed a microarray expression analysis on cortex RNA isolated from anti-*let-7* treated mice and vehicle-treated mice. Upon gene set enrichment analysis of this microarray expression data, we found that the *let-7* target gene ontology group was ranked as the most significantly altered gene ontology group ($P < 10^{-12}$, MSigDb, v3.86) (Subramanian et al., 2005), in agreement with a previous study reporting global de-repression of *let-7* targets in the brains of anti-*let-7* treated mice (Koval et al., 2013), validating this reagent for *let-7* inhibition. As the autophagy pathway normally operates at a basal level in the brains of wild-type mice, we selected Huntington's disease (HD) N171-82Q mice for anti-*let-7* treatment, since HD mouse and fly models have been shown to display prominent autophagy pathway induction (Ravikumar et al., 2004), leading us to hypothesize that anti-*let-7* repression of autophagy would be best detected in the CNS of HD mice. After performing intracerebroventricular injections of anti-*let-7* on adult HD N171-82Q mice, we obtained protein lysates from cortex and hippocampus. LC3 immunoblot analysis revealed reductions in LC3-II levels in the CNS of anti-*let-7* treated HD mice (Figure 7A). When we performed immunoblot analysis of p62 protein, we observed increased p62 levels (Figure 7B), which is often indicative of decreased autophagy. These results further indicate that *let-7* can modulate autophagy in the mammalian CNS.

Although our studies of *let-7* were focused on neuronal autophagy, the amino acid sensing pathway is a potent regulator of mTORC1 complex activation and autophagy outside the CNS (Efeyan et al., 2013). To evaluate the physiological effect of *let-7* repression on peripheral metabolic processes, we performed intraperitoneal injections of anti-*let-7* into mice, and found that anti-*let-7* treated mice exhibited rapid, significant weight gain in comparison to controls treated with scrambled anti-miR, whether on a normal or high-fat diet (Figures 7C and S7A).

Analysis of lean mass and fat mass in anti-*let-7* treated mice reared on a high-fat diet revealed that peripheral *let-7* inhibition resulted in proportionate increases in lean mass and fat mass (Figure S7B–C). Furthermore, as plasma growth hormone and IGF-1 levels do not change in anti-*let-7* treated mice (Figure S7D–E), the increased body weight observed in anti-*let-7* treated mice could not be attributed to effects on the IGF-1 / growth hormone axis. To determine the effect of peripheral anti-*let-7* treatment on autophagy activation status, we quantified GFP-LC3 puncta formation and noted significant decreases in GFP-LC3 puncta counts in muscle and white fat (Figures 7D–G and S7F–G). Hence, *let-7* represses autophagy and promotes weight gain in anti-*let-7* treated mice, suggesting a prominent role for *let-7* in nutrient homeostasis and autophagy pathway control outside the CNS, as well.

DISCUSSION

Pathways of nutrient sensing and metabolic regulation have emerged as powerful determinants of lifespan and healthspan in a wide range of model organisms (Lopez-Otin et

al., 2013). Hence, it comes as no surprise that the genes comprising these pathways are among the most highly conserved genes found in multicellular organisms. The mTOR signaling pathway is especially well conserved, owing to its central role in the integration of cellular homeostasis, and it is the activation state of the mTOR complexes, mTORC1 and mTORC2, that primarily determine the metabolic disposition of the cell. The mTORC1 complex is principally responsible for dictating whether the cell is in an anabolic or catabolic state, and directly regulates energy metabolism, protein synthesis, lipid synthesis, and the autophagy-lysosome pathway (Laplante and Sabatini, 2012). Of the various inputs to the mTORC1 complex, a deficiency of amino acids can outweigh pro-growth signals coming from mitogen or hormone responsive pathways, resulting in mTORC1 inhibition (Smith et al., 2005). Until recently, components of this amino acid sensing pathway were ill-defined, but over the last decade, the principal factors involved in transmission of amino acid satiety to the mTORC1 complex have been delineated, and include a family of highly conserved Ras-related GTP-binding proteins, known collectively as the Ragulator complex, and a set of five proteins, LAMTOR 1, 2, 3, 4 and 5, that anchor the mTORC1 complex at the lysosome (Bar-Peled et al., 2012; Jewell et al., 2013; Kim et al., 2008; Yan and Lamb, 2012). Here, we demonstrate that a highly conserved miRNA, *let-7*, regulates the expression and activity of the genes that encode these and other components of the amino acid sensing pathway, thereby establishing *let-7* as a key node in the mTORC1 regulatory circuit.

To define regulatory factors that control autophagy activity in the CNS, we developed a nutrient deprivation protocol in which primary cortical neurons exposed to nutrient-limited media (NLM) were found to undergo autophagy induction in a mTOR and insulin signaling pathway dependent manner (Young et al., 2009). When we interrogated the transcriptomes of primary neurons subjected to NLM treatment, we noted that multiple members of the *let-7* family exhibited marked up-regulation, and found that Dicer is required for neuronal autophagy activation upon NLM treatment. We then confirmed that *let-7* is sufficient for neuronal autophagy induction in primary neurons transfected with *let-7* mimic. As *let-7* directly targets Dicer mRNA for degradation, and autophagy can degrade Dicer in transformed HeLa cells via the selective autophagy receptor NDP52 (Gibbings et al., 2012), *let-7* – autophagy and Dicer may comprise a negative feedback regulatory loop.

A recurrent theme in miRNA regulation is the observation that an individual miRNA typically achieves a biological effect by targeting multiple genes along a pathway (Small and Olson, 2011). Our analysis of amino acid sensing pathway genes revealed evidence for *let-7* modulation of virtually all the genes that we examined. Indeed, we found *let-7* seed site matches in 13 of 14 amino acid sensing pathway genes, and upon direct evaluation of *let-7* repression of a luciferase reporter linked to these putative target sites, we documented significant reductions in luciferase activity for 11 of 13 tested gene sequences, with strong trends evident for the remaining two genes. Mutation of the seed sites for four target sequences abrogated *let-7* repression in this assay. Moreover, we found that a majority of amino acid sensing pathway genes exhibit significant expression reductions in primary neurons infected with *let-7* expressing lentivirus. In these studies, we aimed for modest levels of *let-7* over-expression, with increases of only 20% – 50%, which corresponds closely to physiological *let-7* induction noted upon nutrient deprivation or amino acid

starvation. Furthermore, we confirmed that *let-7* regulation of target gene expression occurs at the protein level by performing Western blot analysis on anti-*let-7*-treated neuronal cells. Hence, multiple independent assays corroborate *let-7* regulation of amino acid sensing pathway gene expression.

To confirm the physiological importance of *let-7* for autophagy regulation, we determined if neuronal autophagy induction upon NLM treatment required *let-7*, and documented reduced autophagy activation upon anti-*let-7* treatment. When we considered the seed site sequences of *let-7* target genes on the amino acid sensing pathway, we noted that seed site sequences within two target genes, RagD and Map4k3, are perfectly conserved between mammalian species, and for Map4k3 down to zebrafish and frog. This degree of conservation led us to test if knockdown of such targets would be sufficient to induce neuronal autophagy, and we found that either RagD knock-down or Map4k3 knock-down could promote significant autophagy activation in neurons. While these autophagy pathway effects are consistent with autophagy activation upon Slc1a5 knock-down in non-neuronal cells and autophagy repression by a constitutively active RagA mutant in *Drosophila* and in neonatal mice (Efeyan et al., 2013; Kim et al., 2008; Nicklin et al., 2009), our results demonstrate the physiological relevance of amino acid sensing pathway regulation for autophagy modulation in the CNS.

Our discovery of amino acid sensing pathway gene regulation by *let-7* reinforces an emerging view of *let-7* as a predominant regulator of the mTORC1 complex. In a study that examined the regulation of glucose metabolism, *let-7* suppressed the expression of genes encoding components of the insulin signaling pathway in muscle (Zhu et al., 2011). For both the insulin signaling pathway in muscle and the amino acid sensing pathway in neurons, *let-7* regulation yields only modest reductions in expression for individual target genes. Hence, for metabolic pathways, coordinate down-regulation of multiple genes lying on the same pathway likely represents a powerful strategy for achieving a desired metabolic outcome, since network components are often wired into feedback circuit loops. Furthermore, if *let-7* does dictate activity status for the amino acid sensing pathway and the insulin signaling pathway, then this would facilitate consistency of inputs to the mTORC1 complex through a single master genetic switch, increasing the rapidity and efficiency of mTORC1 signal integration. To establish that *let-7* is acting upstream of mTORC1 to mediate its autophagy regulatory effects, we documented that *let-7* induction of autophagy in neurons can be markedly blunted by co-expression of the constitutively active Rheb-Q64L mutant, which promotes mTORC1 complex activation (Inoki et al., 2003). As Rag GTPases, which are targeted by *let-7*, were recently found to regulate the mTORC1 complex in response to both glucose and amino acid status (Efeyan et al., 2013), a requirement for *let-7* to permit autophagy induction in response to either glucose deprivation or amino acid starvation is consistent with these recent findings. Indeed, our results, together with studies of *let-7* regulation of the insulin signaling pathway (Zhu et al., 2011), strongly suggest that *let-7* plays a central role in nutrient homeostasis. A complete understanding of this regulatory circuit, including the pathway by which nutrient stress promotes *let-7* activation, will be an important goal for future studies.

One compelling aspect of this investigation was demonstration of a physiological role for *let-7* in autophagy modulation and metabolism via mTORC1 regulation, though mTORC1-independent metabolic regulation of autophagy could also be involved. Delivery of *let-7* to the striatum of mice co-injected with lentivirus encoding mutant ataxin-3 was sufficient to reduce neuronal protein aggregation, in the context of significantly upregulated LC3-II levels, revealing the ability of *let-7* to promote the degradation of misfolded proteins. Correspondingly, delivery of *let-7* anti-miR to the CNS of HD mice yielded significant repression of autophagy, based upon LC3 and p62 immunoblot analysis. Although these findings indicate that *let-7* is directly regulating autophagy in the CNS, it is also possible that *let-7* modulation achieves these effects by disrupting protein synthesis or other pathways. Hence, further *in vivo* study of *let-7* action on both metabolic and catabolic pathways will be required before one can definitively conclude that *let-7* alone is capable of autophagy induction in the CNS. We also evaluated *let-7* regulation outside the CNS, and we found that, upon peripheral delivery of *let-7* anti-mir, mice experienced rapid weight gain in association with autophagy repression – a finding that is reminiscent of a recent study in which TFEB over-expression in liver rescued obesity and metabolic syndrome in an autophagy-dependent manner (Settembre et al., 2013), and consistent with growth retardation, hyperglycemia, and glucose intolerance in mice over-expressing *let-7g* (Zhu et al., 2011). In light of our results demonstrating *let-7* activation of autophagy, the mechanistic basis of other *let-7* effects also deserve consideration, including *let-7*'s established role as a tumor suppressor (Johnson et al., 2005; Mayr et al., 2007).

One final question worthy of consideration is: Why would amino acid status serve as a potent signal for autophagy regulation in the CNS? Glutamine and leucine are neutral amino acids subject to uptake by a variety of amino acid transporters in neurons, including the broad specificity uncharged (0) amino acid (B^0AT) family (Zaia and Reimer, 2009). B^0AT3 is a neutral amino acid transporter with a very high affinity for leucine, and localizes to synaptic regions where uptake of leucine becomes maximal during periods of intense neuronal activity (Zaia and Reimer, 2009). Hence, as full activation of the amino acid sensing pathway occurs when leucine is exchanged for glutamine, which is produced from glutamate and is thus highly abundant in the CNS (McGale et al., 1977), synaptic and metabolic processes may converge in neurons to dictate autophagy pathway levels via mTORC1 activation state, downstream of neutral amino acid inputs. Consequently, *let-7* suppression of amino acid sensing pathway components in neurons could be highlighting synaptic-metabolic crosstalk at work in the neuronal milieu. Indeed, recent studies have shown that glutamine synthetase potently inhibits autophagy by driving the production of glutamine, which prevents the mTORC1 complex from localizing to lysosomes (van der Vos et al., 2012), where its activation by the Ragulator and LAMTOR complexes occurs (Bar-Peled et al., 2012; Sancak et al., 2010). In addition to being coupled to glutamine efflux, synaptic regulation of leucine transporter action may compete with glutamine synthetase to dictate mTORC1 activation state by favoring leucyl-tRNA synthetase activation of mTORC1 via Ragulator and LAMTOR complexes (Han et al., 2012). Delineation of *let-7* targeting of the amino acid sensing pathway has thus uncovered a robust regulatory network that could be amenable to manipulation for therapeutic benefit in diseases affecting both the CNS and peripheral tissues.

EXPERIMENTAL PROCEDURES

Primary neuron studies

Primary cortical neurons were cultured from postnatal day 0 (P0) C57BL/6J mice or GFP-LC3 transgenic mice (Mizushima et al., 2004). The primary neurons were prepared as described (Young et al., 2009). On day 4 after cell seeding, primary neurons were subjected to siRNA transfection, mimic transfection, anti-miR transfection, or lentiviral infection. On day 5, primary neurons were cultured in complete media (CM), nutrient-limited media (NLM), or amino acid deprivation media (Earle's balanced salt solution, EBSS) for specific time courses, as described (Young et al., 2009). For mimic transfections, CM and NLM controls were run both with or without scrambled mimic control. For siRNA knock-down experiments, primary neurons were transfected with Silencer Select pre-designed siRNA's using RNAi Max (Invitrogen). For mimic transfections, primary neurons were transfected with a stabilized miRNA mimic oligonucleotide *let-7* or a scrambled miR-*let-7* negative control, containing a 6 bp mismatch in the seed site (Dharmacon). The mimic negative control was used in all transfections, along with a siGLO red indicator to monitor transfection efficiency (Dharmacon). RT-PCR analysis of mimic-transfected cells revealed a 4 – 10-fold increase in the expression level of the corresponding mature miRNA. For anti-miR transfections, primary neurons were transfected with 4 μg (6-well) or 1.6 μg (12-well) of a '2'-F/MOE modified anti-miR complementary to *let-7* (Regulus Therapeutics) using Lipofectamine 2000 (Invitrogen).

Luciferase assays

Putative *let-7* regulatory sites in amino acid sensing pathway genes were cloned from mouse cDNA libraries prepared from: (1) wild-type mouse brain; (2) wild-type postnatal day 3 primary cortical neurons; or (3) mouse genomic DNA (gDNA; Promega). For cDNA synthesis, total RNA was extracted using TRIZOL, and cDNA synthesized using SuperScript III first-strand synthesis system for RT-PCR with random hexamer primers (Invitrogen). Regions containing predicted *let-7* binding sites are given in Supplementary Experimental Procedures. PCR amplicons were directionally cloned into the 3'UTR of Renilla luciferase in the psiCHECK-2 dual luciferase plasmid (Promega), using *Xho* I and *Not* I restriction enzymes. PCR products were ligated using T4 DNA ligase (NEB) for 30 min at RT and transformed into DH5α competent *E. coli* cells (Invitrogen). Plasmid DNAs were obtained using QIAprep Miniprep (QIAGEN), and sequenced. For dual luciferase experiments, HEK293T cells were co-transfected with 20 ng of psiCHECK-2 plasmid and 15 or 30 nM of miRVana miRNA mimic negative control #1 (#4464058), or mimic hsa-let-7f-5p (#4464066) using Lipofectamine 2000 (Invitrogen). Changes in relative luciferase were measured 24 hrs later using the dual-luciferase reporter assay system (Promega), and quantified in triplicate using a Promega 96-well plate luminometer. Luciferase experiments were performed in triplicate, and are shown as relative luciferase units (RLU) after normalization of Renilla luciferase to endogenous firefly luciferase, and are shown relative to read-outs obtained with mimic negative-control treated samples.

Autophagy assays

For autophagic induction in GFP-LC3 primary neurons, cells were scored as positive when >5 green puncta were observed. Cell counting for primary neurons was performed, using a Zeiss LSM 780 Observer.Z1 with Zen 2011 LSM 780 software, and only puncta superimposed on soma or within neurite processes were counted for at least 100 cells, from at least three fields / transfection, per experiment. For autophagic flux determination based on LC3 immunoblotting, we measured LC3-II and actin levels by densitometry using NIH ImageJ, and divided LC3-II:actin in the presence of NH4Cl by LC3-II:actin at baseline. For autophagic flux determination in Neuro2a cells and primary cortical neurons transfected with the mCherry-GFP-LC3 vector, we performed confocal imaging as above, categorized puncta as yellow (autophagosomes) or red (autolysosomes), imaged ≥ 100 cells per experimental condition from at least three fields / transfection, and performed at least three separate experiments per condition.

Statistical analysis

All data were prepared for analysis with standard spread sheet software (Microsoft Excel). Statistical analysis was done using Microsoft Excel, Prism 5.0 (Graph Pad), or the VassarStats website < http://faculty.vassar.edu/lowry/VassarStats.html>. For ANOVA, if statistical significance ($p < 0.05$) was achieved, we performed post-hoc analysis to account for multiple comparisons. The level of significance (alpha) was always set at 0.05.

Supplementary Material

Refer to Web version on PubMed Central for supplementary material.

Acknowledgments

We thank J.E. Young, T. Bammler, R.P. Beyer, E. Lopez, and S. Mayo for technical assistance. We are grateful to T. Johansen for the gift of the mCherry-GFP-LC3 plasmid, and Z. Yue for providing the GFP-LC3 transgenic mice, with permission from N. Mizushima. This work was supported by grants from N.I.H. (R01 AG03382 and R01 EY014997 to A.R.L.; T32 AG000216 to A.N.D.; T32 GM008666 to C.L.H.; and P30 HD002274 to the UW CHDD), and the Portuguese Foundation for Science & Technology (SFRH/BPD/87552/2012 to S.D. and E-Rare4/0003/2012 to L.P.A.).

REFERENCES

Bar-Peled L, Schweitzer LD, Zoncu R, Sabatini DM. Ragulator is a GEF for the rag GTPases that signal amino acid levels to mTORC1. Cell. 2012; 150:1196–1208. [PubMed: 22980980]

Boya P, Reggiori F, Codogno P. Emerging regulation and functions of autophagy. Nat Cell Biol. 2013; 15:713–720. [PubMed: 23817233]

Chi SW, Zang JB, Mele A, Darnell RB. Argonaute HITS-CLIP decodes microRNA-mRNA interaction maps. Nature. 2009; 460:479–486. [PubMed: 19536157]

Efeyan A, Zoncu R, Chang S, Gumper I, Snitkin H, Wolfson RL, Kirak O, Sabatini DD, Sabatini DM. Regulation of mTORC1 by the Rag GTPases is necessary for neonatal autophagy and survival. Nature. 2013; 493:679–683. [PubMed: 23263183]

Fineberg SK, Kosik KS, Davidson BL. MicroRNAs potentiate neural development. Neuron. 2009; 64:303–309. [PubMed: 19914179]

Ganley IG, Lam du H, Wang J, Ding X, Chen S, Jiang X. ULK1.ATG13.FIP200 complex mediates mTOR signaling and is essential for autophagy. J Biol Chem. 2009; 284:12297–12305. [PubMed: 19258318]

Gibbings D, Mostowy S, Jay F, Schwab Y, Cossart P, Voinnet O. Selective autophagy degrades DICER and AGO2 and regulates miRNA activity. Nat Cell Biol. 2012; 14:1314–1321. [PubMed: 23143396]

Han JM, Jeong SJ, Park MC, Kim G, Kwon NH, Kim HK, Ha SH, Ryu SH, Kim S. Leucyl-tRNA synthetase is an intracellular leucine sensor for the mTORC1-signaling pathway. Cell. 2012; 149:410–424. [PubMed: 22424946]

Hosokawa N, Hara T, Kaizuka T, Kishi C, Takamura A, Miura Y, Iemura S, Natsume T, Takehana K, Yamada N, et al. Nutrient-dependent mTORC1 association with the ULK1-Atg13-FIP200 complex required for autophagy. Mol Biol Cell. 2009; 20:1981–1991. [PubMed: 19211835]

Inoki K, Li Y, Xu T, Guan KL. Rheb GTPase is a direct target of TSC2 GAP activity and regulates mTOR signaling. Genes Dev. 2003; 17:1829–1834. [PubMed: 12869586]

Jewell JL, Russell RC, Guan KL. Amino acid signalling upstream of mTOR. Nat Rev Mol Cell Biol. 2013; 14:133–139. [PubMed: 23361334]

Johnson SM, Grosshans H, Shingara J, Byrom M, Jarvis R, Cheng A, Labourier E, Reinert KL, Brown D, Slack FJ. RAS is regulated by the let-7 microRNA family. Cell. 2005; 120:635–647. [PubMed: 15766527]

Kim E, Goraksha-Hicks P, Li L, Neufeld TP, Guan KL. Regulation of TORC1 by Rag GTPases in nutrient response. Nat Cell Biol. 2008; 10:935–945. [PubMed: 18604198]

Klionsky DJ, Abdalla FC, Abeliovich H, Abraham RT, Acevedo-Arozena A, Adeli K, Agholme L, Agnello M, Agostinis P, Aguirre-Ghiso JA, et al. Guidelines for the use and interpretation of assays for monitoring autophagy. Autophagy. 2012; 8:445–544. [PubMed: 22966490]

Koval ED, Shaner C, Zhang P, du Maine X, Fischer K, Tay J, Chau BN, Wu GF, Miller TM. Method for widespread microRNA-155 inhibition prolongs survival in ALS-model mice. Hum Mol Genet. 2013; 22:4127–4135. [PubMed: 23740943]

Laplante M, Sabatini DM. mTOR signaling in growth control and disease. Cell. 2012; 149:274–293. [PubMed: 22500797]

Lipinski MM, Hoffman G, Ng A, Zhou W, Py BF, Hsu E, Liu X, Eisenberg J, Liu J, Blenis J, et al. A genome-wide siRNA screen reveals multiple mTORC1 independent signaling pathways regulating autophagy under normal nutritional conditions. Dev Cell. 2010; 18:1041–1052. [PubMed: 20627085]

Lopez-Otin C, Blasco MA, Partridge L, Serrano M, Kroemer G. The hallmarks of aging. Cell. 2013; 153:1194–1217. [PubMed: 23746838]

Mayr C, Hemann MT, Bartel DP. Disrupting the pairing between let-7 and Hmga2 enhances oncogenic transformation. Science. 2007; 315:1576–1579. [PubMed: 17322030]

McGale EH, Pye IF, Stonier C, Hutchinson EC, Aber GM. Studies of the inter-relationship between cerebrospinal fluid and plasma amino acid concentrations in normal individuals. J Neurochem. 1977; 29:291–297. [PubMed: 886334]

Mizushima N, Komatsu M. Autophagy: renovation of cells and tissues. Cell. 2011; 147:728–741. [PubMed: 22078875]

Mizushima N, Noda T, Yoshimori T, Tanaka Y, Ishii T, George MD, Klionsky DJ, Ohsumi M, Ohsumi Y. A protein conjugation system essential for autophagy. Nature. 1998; 395:395–398. [PubMed: 9759731]

Mizushima N, Yamamoto A, Matsui M, Yoshimori T, Ohsumi Y. In vivo analysis of autophagy in response to nutrient starvation using transgenic mice expressing a fluorescent autophagosome marker. Mol Biol Cell. 2004; 15:1101–1111. [PubMed: 14699058]

Nascimento-Ferreira I, Nobrega C, Vasconcelos-Ferreira A, Onofre I, Albuquerque D, Aveleira C, Hirai H, Deglon N, Pereira de Almeida L. Beclin 1 mitigates motor and neuropathological deficits in genetic mouse models of Machado-Joseph disease. Brain. 2013; 136:2173–2188. [PubMed: 23801739]

Nicklin P, Bergman P, Zhang B, Triantafellow E, Wang H, Nyfeler B, Yang H, Hild M, Kung C, Wilson C, et al. Bidirectional transport of amino acids regulates mTOR and autophagy. Cell. 2009; 136:521–534. [PubMed: 19203585]

Paulson HL, Perez MK, Trottier Y, Trojanowski JQ, Subramony SH, Das SS, Vig P, Mandel JL, Fischbeck KH, Pittman RN. Intranuclear inclusions of expanded polyglutamine protein in spinocerebellar ataxia type 3. Neuron. 1997; 19:333–344. [PubMed: 9292723]

Ravikumar B, Vacher C, Berger Z, Davies JE, Luo S, Oroz LG, Scaravilli F, Easton DF, Duden R, O'Kane CJ, et al. Inhibition of mTOR induces autophagy and reduces toxicity of polyglutamine expansions in fly and mouse models of Huntington disease. Nat Genet. 2004; 36:585–595. [PubMed: 15146184]

Roczniak-Ferguson A, Petit CS, Froehlich F, Qian S, Ky J, Angarola B, Walther TC, Ferguson SM. The transcription factor TFEB links mTORC1 signaling to transcriptional control of lysosome homeostasis. Sci Signal. 2012; 5:ra42. [PubMed: 22692423]

Roush S, Slack FJ. The let-7 family of microRNAs. Trends Cell Biol. 2008; 18:505–516. [PubMed: 18774294]

Sancak Y, Bar-Peled L, Zoncu R, Markhard AL, Nada S, Sabatini DM. Ragulator-Rag complex targets mTORC1 to the lysosomal surface and is necessary for its activation by amino acids. Cell. 2010; 141:290–303. [PubMed: 20381137]

Sancak Y, Peterson TR, Shaul YD, Lindquist RA, Thoreen CC, Bar-Peled L, Sabatini DM. The Rag GTPases bind raptor and mediate amino acid signaling to mTORC1. Science. 2008; 320:1496–1501. [PubMed: 18497260]

Scott SV, Hefner-Gravink A, Morano KA, Noda T, Ohsumi Y, Klionsky DJ. Cytoplasm-to-vacuole targeting and autophagy employ the same machinery to deliver proteins to the yeast vacuole. Proc Natl Acad Sci U S A. 1996; 93:12304–12308. [PubMed: 8901576]

Settembre C, De Cegli R, Mansueto G, Saha PK, Vetrini F, Visvikis O, Huynh T, Carissimo A, Palmer D, Klisch TJ, et al. TFEB controls cellular lipid metabolism through a starvation-induced autoregulatory loop. Nat Cell Biol. 2013; 15:647–658. [PubMed: 23604321]

Settembre C, Di Malta C, Polito VA, Garcia Arencibia M, Vetrini F, Erdin S, Erdin SU, Huynh T, Medina D, Colella P, et al. TFEB links autophagy to lysosomal biogenesis. Science. 2011; 332:1429–1433. [PubMed: 21617040]

Settembre C, Zoncu R, Medina DL, Vetrini F, Erdin S, Huynh T, Ferron M, Karsenty G, Vellard MC, Facchinetti V, et al. A lysosome-to-nucleus signalling mechanism senses and regulates the lysosome via mTOR and TFEB. Embo J. 2012; 31:1095–1108. [PubMed: 22343943]

Shintani T, Klionsky DJ. Autophagy in health and disease: a double-edged sword. Science. 2004; 306:990–995. [PubMed: 15528435]

Small EM, Olson EN. Pervasive roles of microRNAs in cardiovascular biology. Nature. 2011; 469:336–342. [PubMed: 21248840]

Smith EM, Finn SG, Tee AR, Browne GJ, Proud CG. The tuberous sclerosis protein TSC2 is not required for the regulation of the mammalian target of rapamycin by amino acids and certain cellular stresses. J Biol Chem. 2005; 280:18717–18727. [PubMed: 15772076]

Subramanian A, Tamayo P, Mootha VK, Mukherjee S, Ebert BL, Gillette MA, Paulovich A, Pomeroy SL, Golub TR, Lander ES, et al. Gene set enrichment analysis: a knowledge-based approach for interpreting genome-wide expression profiles. Proc Natl Acad Sci U S A. 2005; 102:15545–15550. [PubMed: 16199517]

van der Vos KE, Eliasson P, Proikas-Cezanne T, Vervoort SJ, van Boxtel R, Putker M, van Zutphen IJ, Mauthe M, Zellmer S, Pals C, et al. Modulation of glutamine metabolism by the PI(3)K-PKB-FOXO network regulates autophagy. Nat Cell Biol. 2012; 14:829–837. [PubMed: 22820375]

Yan L, Lamb RF. Amino acid sensing and regulation of mTORC1. Semin Cell Dev Biol. 2012; 23:621–625. [PubMed: 22342805]

Young JE, Martinez RA, La Spada AR. Nutrient deprivation induces neuronal autophagy, and implicates reduced insulin signaling in neuroprotective autophagy activation. J Biol Chem. 2009; 284:2362–2373.

Zaia KA, Reimer RJ. Synaptic Vesicle Protein NTT4/XT1 (SLC6A17) Catalyzes Na+-coupled Neutral Amino Acid Transport. J Biol Chem. 2009; 284:8439–8448. [PubMed: 19147495]

Zhu H, Shyh-Chang N, Segre AV, Shinoda G, Shah SP, Einhorn WS, Takeuchi A, Engreitz JM, Hagan JP, Kharas MG, et al. The Lin28/let-7 axis regulates glucose metabolism. Cell. 2011; 147:81–94. [PubMed: 21962509]

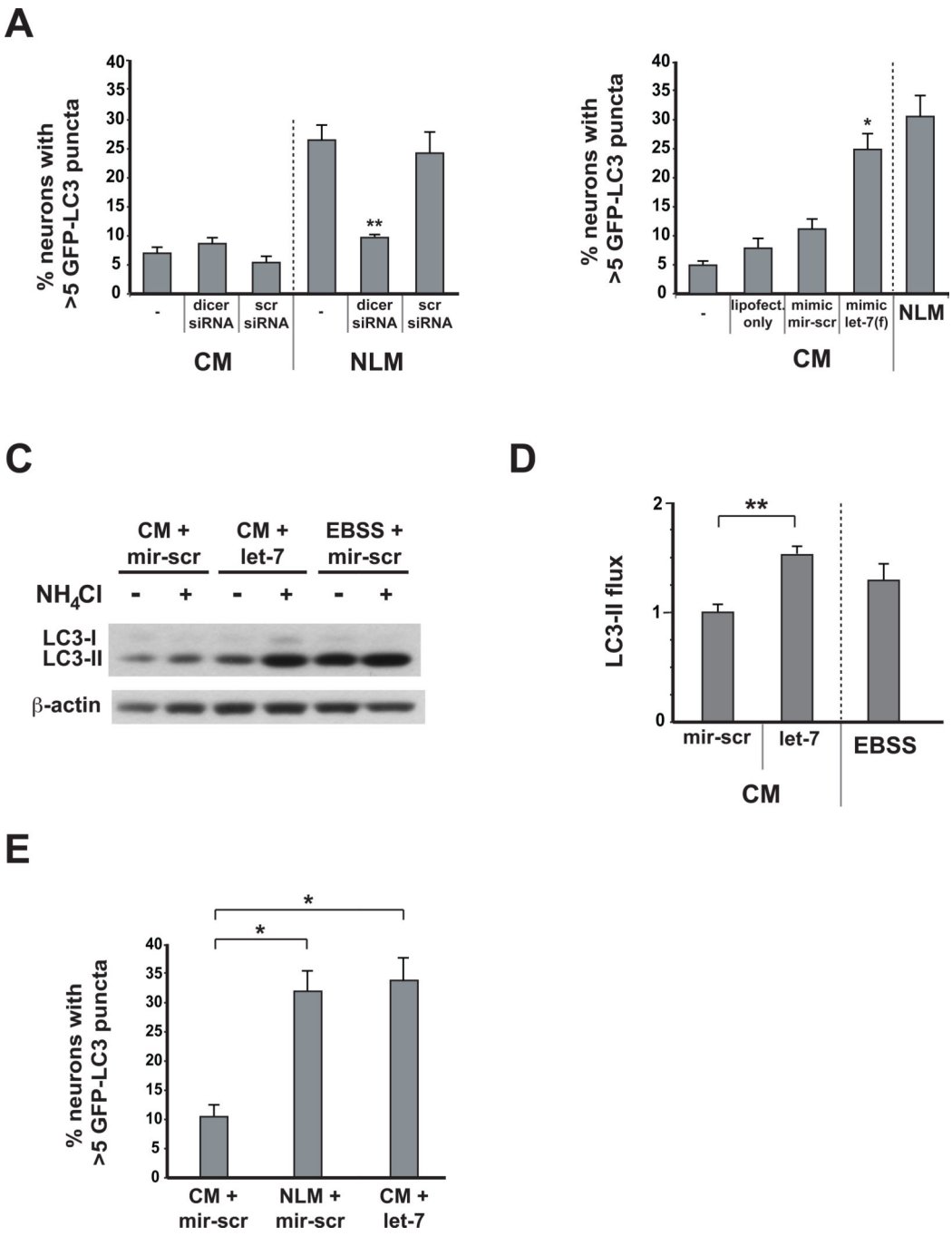

Figure 1. *Let-7* activates the autophagy pathway in neurons

(**A**) GFP-LC3 primary cortical neurons cultured in complete media (CM) or nutrient-limited media (NLM) were transfected with Dicer siRNA, scrambled (scr) siRNA, or mock-transfected (−), and GFP-LC3 puncta / neuron were counted (mean ± s.e.m., $n = 3$ independent experiments).

(**B**) GFP-LC3 primary cortical neurons cultured in CM were transfected with scrambled control mimic (mir-scr) or *let-7* mimic. Untreated CM-cultured neurons and lipofectamine-

treated CM-cultured neurons were negative controls, while NLM treatment served as positive control (mean ± s.e.m., $n = 3$ independent experiments).

(**C**) LC3 immunoblot analysis of GFP-LC3 primary cortical neurons cultured in CM with mir-scr, amino acid deprivation media (EBSS) with mir-scr, or CM with *let-7* mimic, in the absence or presence of the lysosomal inhibitor ammonium chloride.

(**D**) Densitometry analysis of LC3 immunoblotting in (**C**) for autophagic flux quantification (mean ± s.e.m., $n = 4$ independent experiments).

(**E**) NLM control-treated neurons and CM-cultured neurons treated with *let-7* mimic both display significant increases in the number of cells with >5 GFP-LC3 puncta (mean ± s.e.m., $n = 3$ independent experiments).

$^{*}P < .05$, $^{**}P < .01$; ANOVA with post-hoc Tukey test.

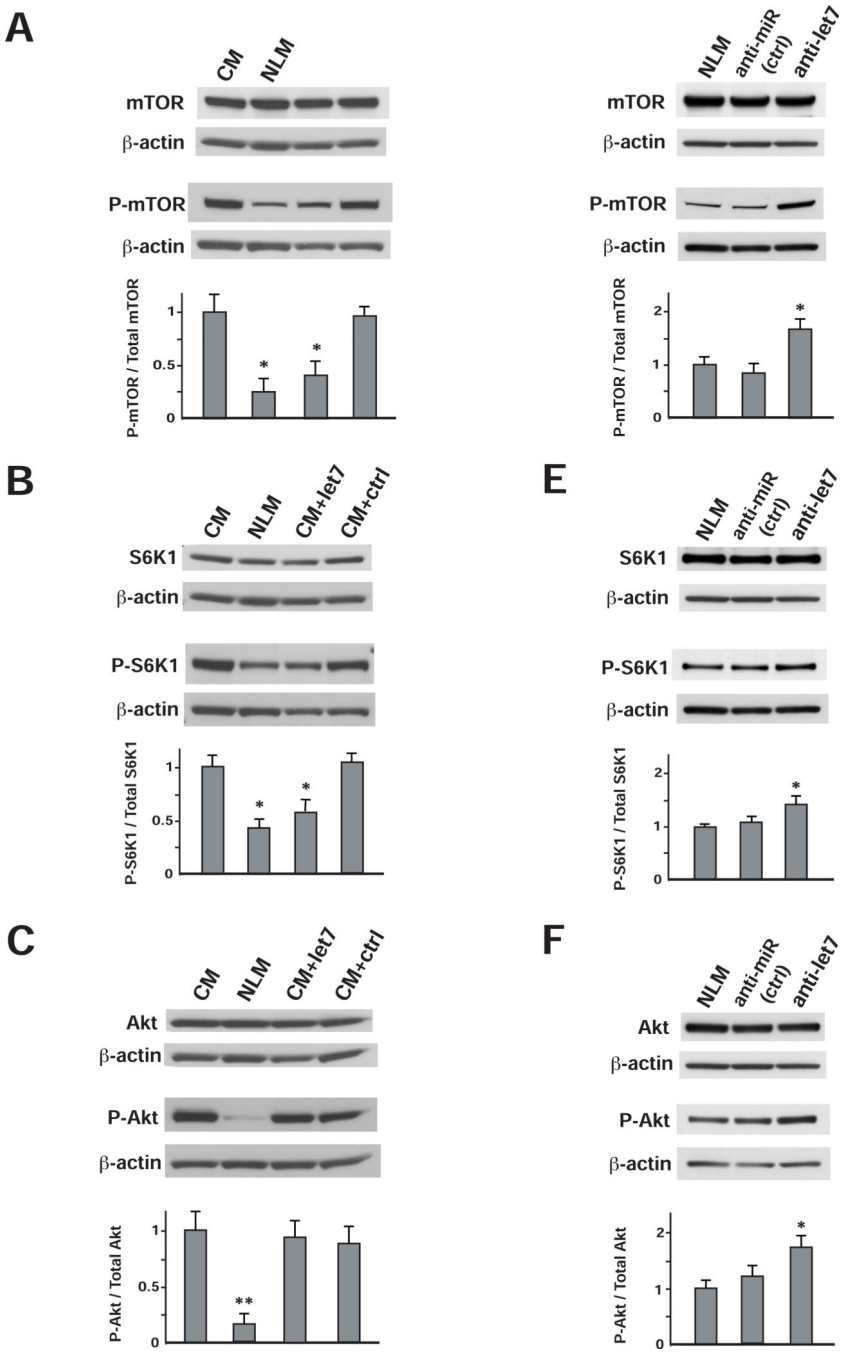

Figure 2. *Let-7* represses mTORC1 without suppressing the insulin signaling pathway

(**A** – **C**) GFP-LC3 primary cortical neurons cultured in CM were transfected with *let-7* mimic, or scrambled control mimic (ctrl), and protein lysates were immunoblotted for indicated proteins. Densitometric quantifications of phospho-mTOR / total mTOR (**A**), phospho-S6K1 / total S6K1 (**B**), and phospho-Akt / total Akt (**C**), all respectively normalized to actin, are shown below respective immunoblots. (**D** – **F**) GFP-LC3 primary cortical neurons cultured in NLM were transfected with anti-miR scrambled control or with anti-*let-7*, and protein lysates were immunoblotted for indicated proteins. Densitometric

quantifications of phospho-mTOR / total mTOR (**D**), phospho-S6K1 / total S6K1 (**E**), and phospho-Akt / total Akt (**F**), all respectively normalized to actin, are shown below respective immunoblots (mean ± s.e.m., $n = 4$ independent experiments). *$P < .05$, **$P < .01$; ANOVA with post-hoc Tukey test.

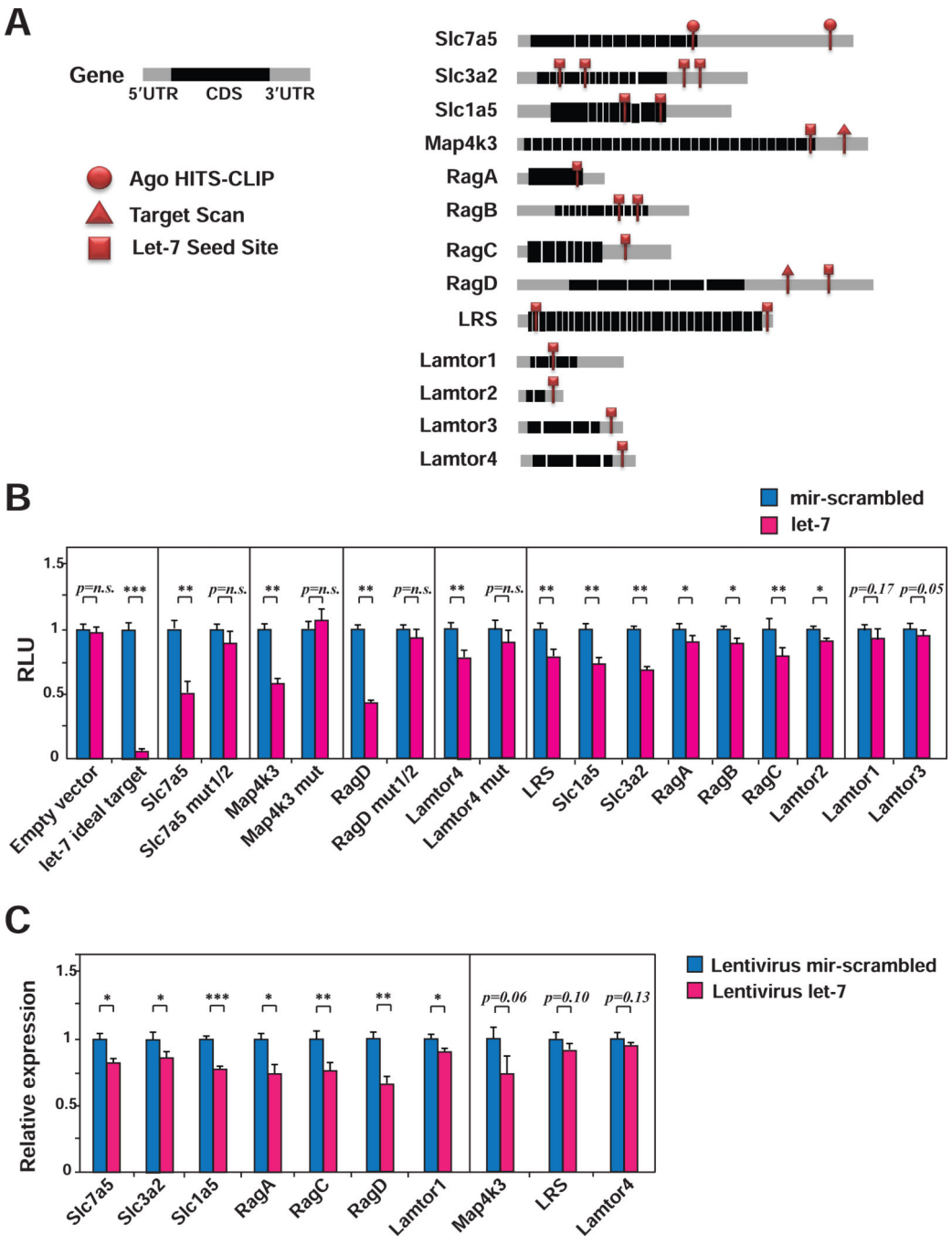

Figure 3. *Let-7* represses expression of amino acid sensing pathway genes

(**A**) Location of *let-7* binding sites within coding regions and 3'UTRs as revealed by argonaute-2 HITS-CLIP (Chi et al., 2009), TargetScan 6.0, or direct scanning for *let-7* seed sites.

(**B**) Luciferase reporter assays were performed by placing 3'UTR sequences or coding region sequences 3' to the luciferase cDNA in the pGL3 vector, and measuring relative luciferase activity in HEK293T cells upon transfection of *let-7* mimic or scrambled miRNA. Relative luciferase activity is shown for *let-7* mimic normalized to miR-scrambled, and the

effect of mutations in seed sequences for a subset of *let-7* targets (Slc7a5, Map4k3, RagD, and Lamtor4) was also measured (mean ± s.e.m., $n = 3$ independent experiments).
(**C**) RT-PCR quantification of amino acid sensing pathway gene expression in primary cortical neurons infected with either *let-7* lentivirus or miR-scrambled lentivirus (mean ± s.e.m., $n = 3$ independent experiments).
$^{*}P < .05$, $^{**}P < .01$, $^{***}P < .001$; t-test.

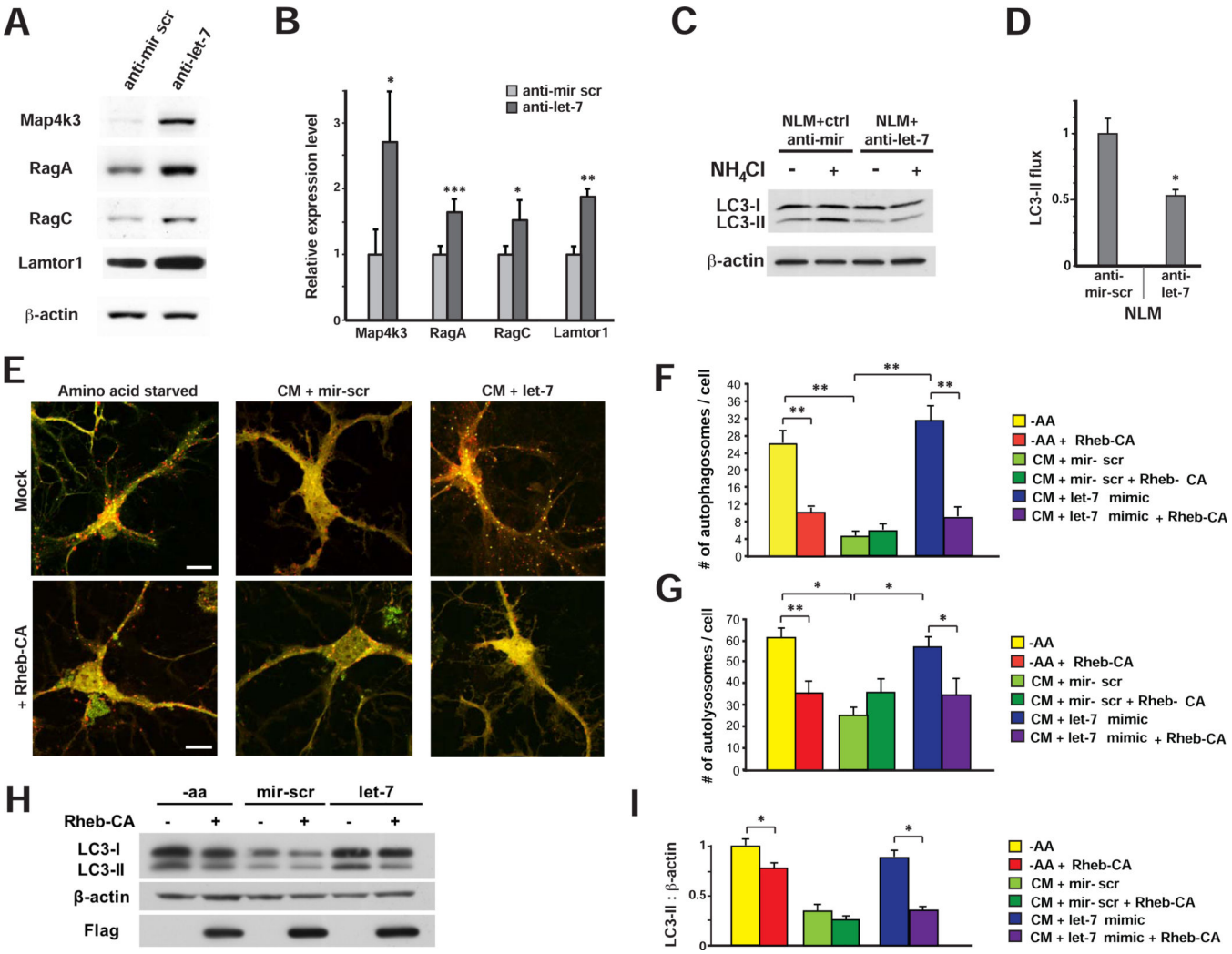

Figure 4. *Let-7* regulation occurs at the protein level and controls autophagy activation upstream of the mTORC1 complex

(**A**) Neuro2a cells were transfected with anti-miR scrambled control or with anti-*let-7*, and whole cell extracts were immunoblotted for the indicated proteins.

(**B**) Densitometric quantification of immunoblot analysis shown in (**A**) (mean ± s.e.m., $n = 3$ independent experiments). *$P < .05$, **$P < .01$, ***$P < .001$; t-test.

(**C**) LC3 immunoblot analysis of primary cortical neurons transfected with anti-miR scrambled control or with anti-*let-7*, and subjected to NLM culture conditions, in the absence or presence of the lysosomal inhibitor ammonium chloride.

(**D**) Densitometry analysis of LC3 immunoblotting in (**C**) for autophagic flux quantification (mean ± s.e.m., $n = 4$ independent experiments). *$P < .05$; t- test.

(**E**) Primary cortical neurons were infected with Flag-Rheb-Q64L lentivirus or mock infected, transfected with GFP-LC3-mCherry vector in combination with scrambled miRNA mimic or *let-7* mimic, and then cultured in EBSS media (amino acid starvation) or in CM. Scale bars = 10 μm

(**F**) Average number of autophagosomes / cell (mean ± s.e.m., $n = 3$ independent experiments) for primary neurons in (**E**).

(**G**) Average number of autolysosomes / cell (mean ± s.e.m., $n = 3$ independent experiments) for primary neurons in (**E**).

(**H**) LC3 immunoblot analysis of primary cortical neurons infected with Flag-Rheb-Q64L lentivirus or mock infected, transfected with scrambled miRNA mimic or *let-7* mimic, and then cultured in EBSS media for amino acid starvation (±aa) or in CM. Success of Rheb-Q64L infection was confirmed by immunoblotting for the Flag epitope.

(**I**) Densitometry quantification of LC3-II, normalized to actin, confirms Rheb-Q64L repression of *let-7*-dependent autophagy activation (mean ± s.e.m., $n = 3$ independent experiments).

*$P < .05$, **$P < .01$; ANOVA with post-hoc Tukey test.

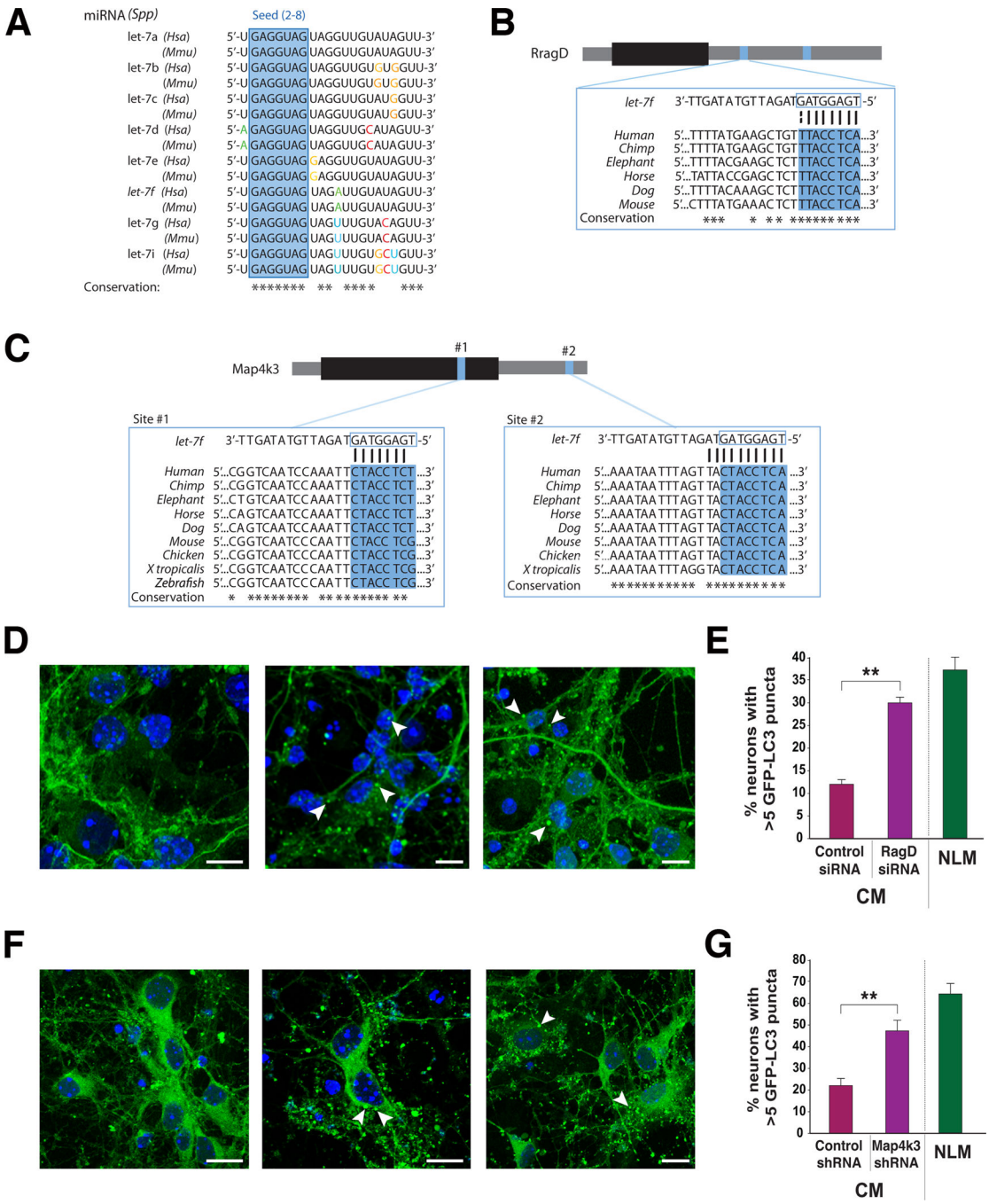

Figure 5. Amino acid sensing pathway components with evolutionarily conserved *let-7* binding sites regulate autophagy in neurons

(**A**) Seed site region sequences for the eight *let-7* family members. Note perfect seed site conservation (blue box). *Hsa = Homo sapiens*; *Mmu = Mus musculus*

(**B**) *let-7* seed site target sequences in the *RagD* 3'UTR are perfectly conserved in mammals.

(**C**) *let-7* seed site target sequences in the *Map4k3* coding region are conserved in mammals and down to zebrafish, while *let-7* seed site target sequences in the *Map4k3* 3'UTR are conserved in mammals and down to frog.

(**D**) GFP-LC3 primary cortical neurons cultured in CM transfected with RagD siRNA exhibit prominent puncta formation (arrowheads), comparable to NLM treatment.
(**E**) Quantification of GFP-LC3 puncta counts / neuron for (**D**). NLM treatment serves as positive control (mean ± s.e.m., $n = 3$ independent experiments).
(**F**) GFP-LC3 primary cortical neurons cultured in CM transfected with Map4k3 shRNA exhibit prominent puncta formation (arrowheads), comparable to NLM treatment.
(**G**) Quantification of GFP-LC3 puncta counts / neuron for (**F**). NLM treatment serves as positive control (mean ± s.e.m., $n = 3$ independent experiments).
$^{**}P < .01$; ANOVA with post-hoc Tukey test. Scale bars = 20 μm

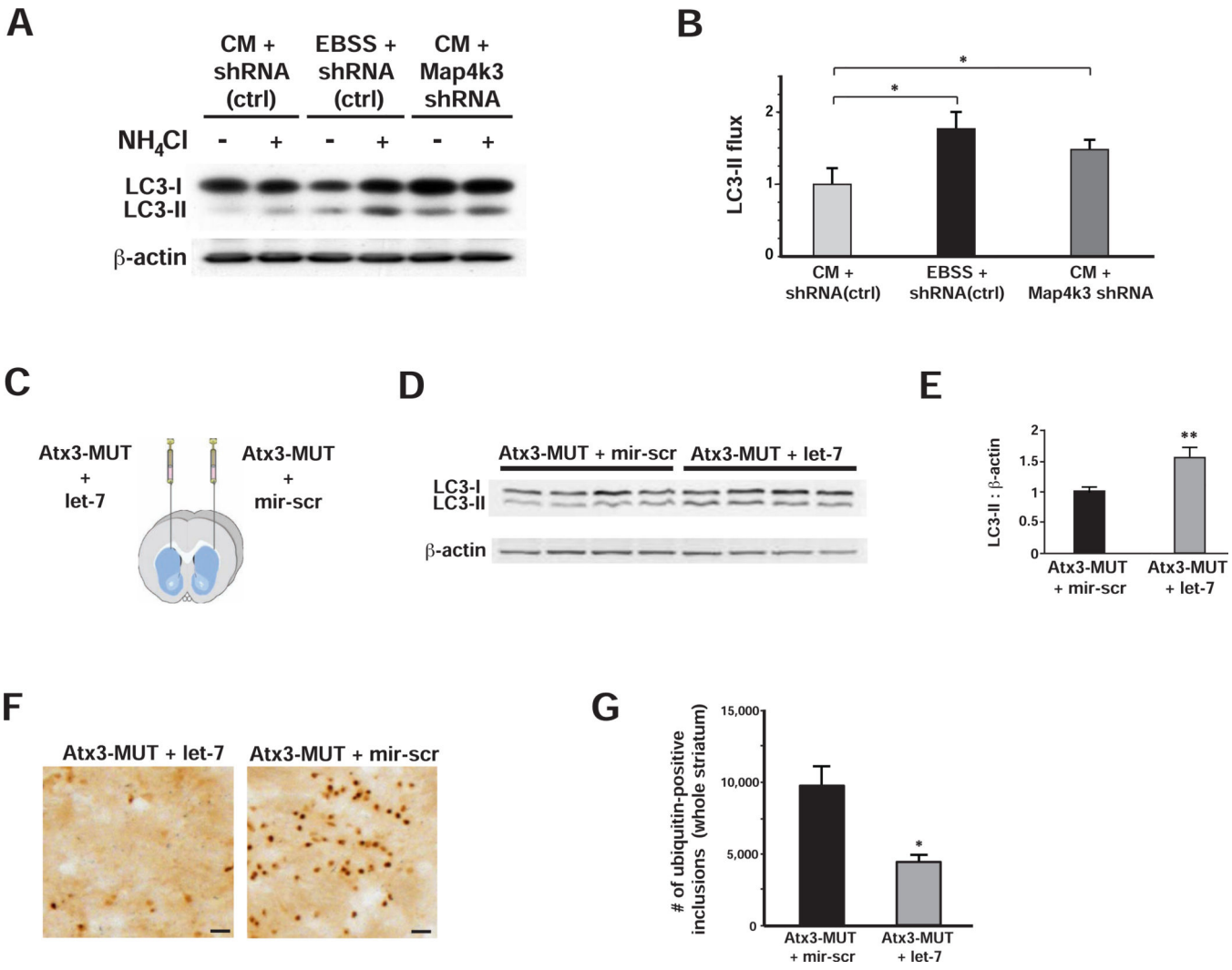

Figure 6. *Let-7* promotes productive autophagy pathway activation in primary neurons and in mouse brain

(**A**) LC3 immunoblot analysis of primary cortical neurons transfected with control shRNA or Map4k3 shRNA, and cultured under CM or amino acid deprivation (EBSS) conditions, in the absence or presence of the lysosomal inhibitor ammonium chloride.

(**B**) Densitometry analysis of LC3 immunoblotting in (**A**) for autophagic flux quantification (mean ± s.e.m., $n = 3$ independent experiments). *$P < .05$, **$P < .01$; ANOVA with post-hoc Tukey test.

(**C**) Schematic representation of stereotactic injection of lentiviral vectors in mouse striatum. Human mutant ataxin-3 with 72 glutamines (Atx3-MUT) was co-injected with *let*-7 in one hemisphere or with mir-scr in the contralateral hemisphere as control.

(**D**) LC3 immunoblot analysis of protein lysates from the striatum of mice four weeks after stereotactic injection.

(**E**) Densitometry analysis of LC3 immunoblotting in (**D**) (mean ± s.e.m., $n = 7$ mice). **$P < .01$; t-test.

(**F**) Ubiquitin immunostaining of striatum sections from mice co-injected with Atx3-MUT and *let-7*, or with Atx3-MUT and mir-scr. Scale bars = 20 μm

(**G**) Quantification of ubiquitin-positive inclusions for whole striatum from mice shown in (**F**) (mean ± s.e.m., $n = 6$ mice). *$P < .05$; t-test.

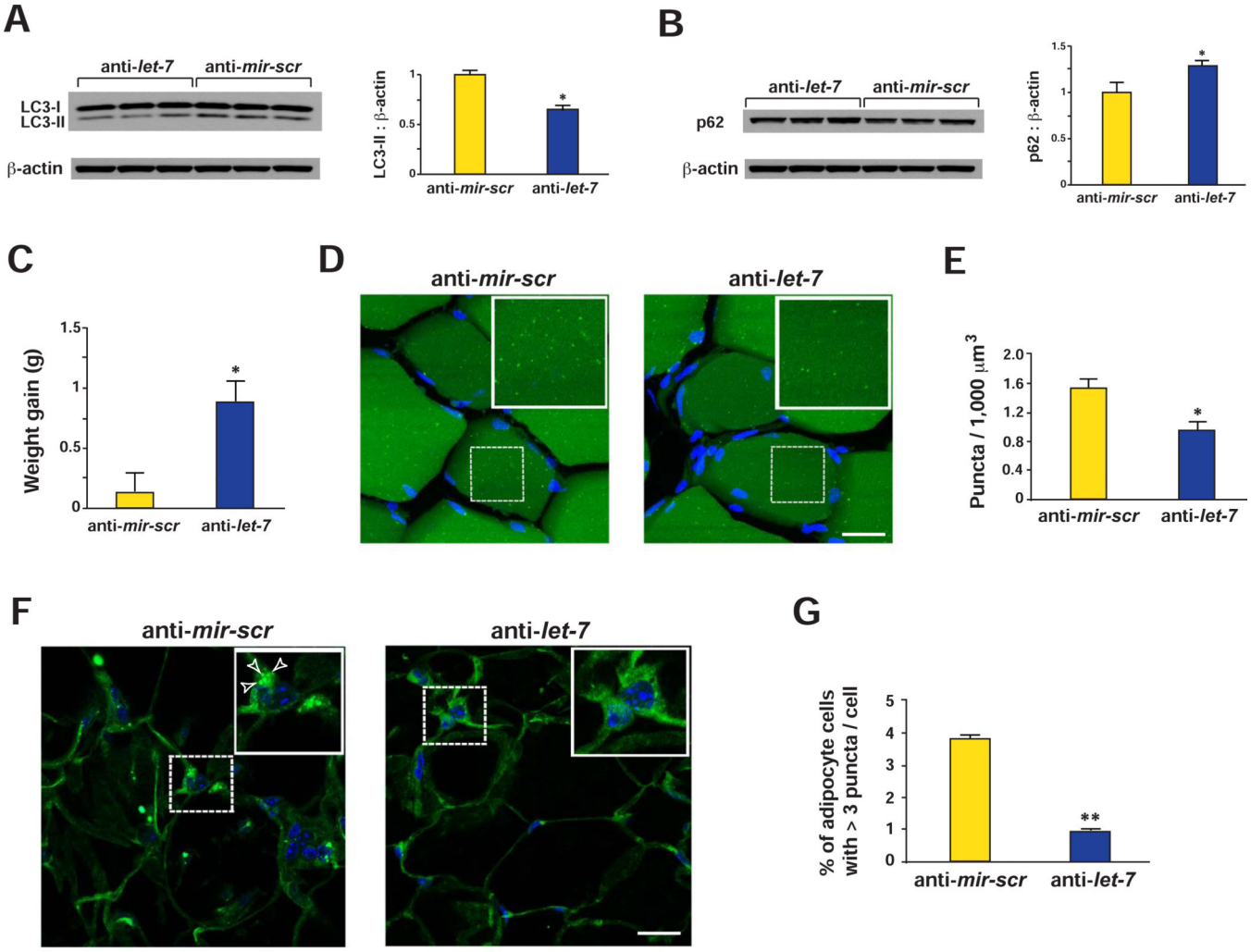

Figure 7. *Let-7* anti-miR treatment suppresses autophagy in CNS and peripheral tissues

(**A**) LC3 immunoblot analysis of protein lysates from the cortex of HD N171-82Q mice two weeks after intracerebroventricular injection of anti-*let-7* or scrambled anti-miR (anti-*mir*-scr). Densitometry analysis indicates a significant reduction in autophagy induction in anti-*let-7* treated mice (mean ± s.e.m., $n = 3$ independent experiments, 3 mice /group).

(**B**) p62 immunoblot analysis of protein lysates from the hippocampus of HD N171-82Q mice two weeks after intracerebroventricular injection of anti-*let-7* or anti-*mir*-scr. Densitometry analysis indicates significant accumulation of p62 in anti-*let-7* treated mice (mean ± s.e.m., $n = 3$ independent experiments, 3 mice / group).

(**C**) GFP-LC3 male transgenic mice received twice weekly intraperitoneal injections of anti-*let-7* or anti-*mir*-scr (5 mg / kg), and were weighed at the end of 28 days (mean ± s.e.m., $n = 3 – 4$ mice /group).

(**D**) Sections of quadriceps muscle from GFP-LC3 male transgenic mice treated with anti-*let-7* or anti-*mir*-scr. Inset: note reduced number of GFP-LC3 puncta in mice treated with anti-*let-7*.

(**E**) Quantification of GFP-LC3 puncta in muscle cells shown in (**D**). GFP-LC3 puncta counts ($n \geq 30$ cylindrical regions / group) are reduced in mice treated with *let-7* anti-miR (mean ± s.e.m., $n = 3 – 4$ mice / group).

(**F**) Sections of epididymal white fat from GFP-LC3 male transgenic mice treated with anti-*let-7* or anti-*mir*-scr. Inset: arrowheads indicate prominent GFP-LC3 puncta in individual white fat cells in mice treated with anti-*mir*-scr.

(**G**) Quantification of GFP-LC3 puncta in white fat cells shown in (**F**). White fat cells exhibiting >3 GFP-LC3 puncta / cell ($n \geq 250$ cells / group) are reduced in mice treated with anti-*let-7* (mean ± s.e.m., $n = 3 – 4$ mice / group).

*$P < .05$, **$P < .01$; t-test. Scale bars = 20 μm